

# Global Positioning System Sensor with Instantaneous-Impact-Point Prediction for Sounding Rockets

Oliver Montenbruck\* and Markus Markgraf†  
DLR, German Aerospace Center, 82234 Wessling, Germany

The development and verification of a dedicated global positioning system (GPS) sensor for sounding rocket missions is described. It is based on the hardware design of a terrestrial low-cost, single-frequency coarse/acquisition (C/A) code receiver but operates an enhanced software that has been specifically adapted for high dynamics applications. Besides the navigation and timing function provided by traditional GPS receivers, the prediction of the instantaneous impact point (IIP) has for the first time been integrated into the receiver software. Making use of a newly developed perturbed-parabolic trajectory model, the receiver can directly perform real-time IIP predictions with an accuracy that is compatible with operational ground software and is only limited by atmospheric forces. It is expected that the availability of onboard IIP prediction will both simplify existing range safety systems and contribute to a future increase of the onboard autonomy of sounding rocket missions. The overall receiver performance is demonstrated with hardware-in-the-loop simulations and actual flight data for representative mission profiles.

## Nomenclature

$d$	=	ground distance of impact point, m
$g$	=	gravitational acceleration, m/s <sup>2</sup>
$g_{\text{eff}}$	=	effective surface acceleration, m/s <sup>2</sup>
$h$	=	height above geoid, m
$h_0$	=	height above geoid at initial epoch, m
$J_2$	=	Earth oblateness coefficient
$R_{\oplus}$	=	Earth radius, m
$s$	=	impact point position, m
$s_0$	=	initial position vector, m
$t_0$	=	initial epoch
$u_{\text{imp}}$	=	vertical impact velocity, m/s
$u_0$	=	initial velocity vector, m/s
$u_{0,E}$	=	east component of $u_0$ , m/s
$u_{0,N}$	=	north component of $u_0$ , m/s
$u_{0,\text{up}}$	=	up component of $u_0$ , m/s
$\Delta s_{\text{IIP}}$	=	correction of impact point position, m
$\lambda$	=	geodetic longitude, deg
$\tau$	=	time to impact, s
$\varphi$	=	geodetic latitude, deg
$\omega_{\oplus}$	=	Earth angular velocity, rad/s

## I. Introduction

**I**N parallel with the tremendous growth of terrestrial and airborne global positioning system (GPS) applications, an ever-increasing number of space missions utilize the global positioning system for navigation and scientific measurements. Likewise, GPS receivers offer numerous prospective benefits onboard a sounding rocket. During the various flight phases, GPS measurements can support range safety monitoring, geolocation and time tagging, event triggering, recovery operations, and, finally, a postmission performance and trajectory analysis.<sup>1,2</sup>

Right after launch GPS position and velocity measurements allow for a rapid recognition of boost and guidance problems through real-time prediction of the instantaneous impact point. This information can directly be used by the range safety officer to decide on the need and feasibility of an abnormal flight termination. In the postmission analysis the GPS navigation data can furthermore be used to compare the actual performance of a boost motor with premission models and to infer the aerodynamic properties of the rocket. This enables a refined planning of future missions based on improved parameter sets. In the subsequent free-flight phase precise position and timing data collected jointly with the science measurements are essential for the study of regional and temporal variations in the atmosphere and magnetosphere and a comparison with experiments performed at other sites. In case of multiple payloads separated during the mission or flown simultaneously on different rockets, GPS can provide highly accurate relative state vectors and timing information for the science data synchronization.<sup>3</sup> Time and position information can likewise be employed to activate experiments and service systems precisely at a desired flight stage. A GPS receiver can thus take over functions traditionally performed by mechanical timers and barometric switches. Finally, the instantaneous payload position measured by a GPS receiver can continuously be relayed to the control center during the final descent and parachute phase to allow a rapid and reliable recovery even in the presence of pronounced wind fields. Aside from a high accuracy of the basic navigation and timing information, which is already available with single-frequency coarse/acquisition (C/A) code receivers, GPS has the additional benefit of an onboard data availability. This offers the prospect of increased autonomy in future rocket systems and can be applied for onboard geocoding or onboard instantaneous impact point (IIP) prediction. Furthermore the overall system cost is considered to be notably lower than that of alternative tracking systems.<sup>4</sup>

All of the aforementioned benefits come at the expense of dedicated enhancements of the GPS receiver design, required to ensure proper tracking at the extreme signal dynamics encountered during the boost phase and reentry. This paper describes the hardware and software of the Orion-HD high-dynamics GPS receiver. It has been adapted by the German Space Operations Center from a prototype for low-cost, mass market applications to the highly specialized use on sounding rockets. Motivated by the needs of its Mobile Rocket Base, which plans, prepares, and performs sounding rocket launches at various international launch sites, a research and development program for GPS tracking systems has been set up in an effort to ultimately replace or minimize conventional radar stations. In a first step the Orion-HD receiver has received basic software extensions

Received 16 April 2003; revision received 7 July 2003; accepted for publication 21 July 2003; presented as Paper 2003-5722 at the AIAA Guidance, Navigation, and Control Conference, Austin, TX, 11 August 2003. Copyright © 2003 by Oliver Montenbruck and Markus Markgraf. Published by the American Institute of Aeronautics and Astronautics, Inc., with permission. Copies of this paper may be made for personal or internal use, on condition that the copier pay the \$10.00 per-copy fee to the Copyright Clearance Center, Inc., 222 Rosewood Drive, Danvers, MA 01923; include the code 0022-4650/04 \$10.00 in correspondence with the CCC.

\*Head, GPS Technology and Navigation Group, German Space Operations Center, Oberpfaffenhofen; oliver.montenbruck@dlr.de.

†Engineer, GPS Technology and Navigation Group, German Space Operations Center, Oberpfaffenhofen; markus.markgraf@dlr.de.

and modifications for high dynamics use<sup>5</sup> and undergone a preliminary flight qualification together with a novel antenna system.<sup>6</sup> In a next step which is addressed by the present report, the system has been upgraded for carrier phase tracking and supplemented by a simple, yet efficient, IIP prediction algorithm. It computes the expected touchdown point of the sounding rocket based on the latest state vector and outputs the result in real time along with the navigation solution. The mathematical formulation of the IIP prediction algorithm, which makes use of a perturbed parabolic trajectory model and can well be applied with limited computing resources, is described in a separate section of this report. Finally, we discuss the overall navigation and IIP prediction performance of the Orion-HD GPS receiver as obtained in ground-based signal simulator tests and actual sounding rocket flights.

## II. GPS Hardware

The GPS Orion receiver, which serves as a platform for the IIP prediction system, has originally been designed by Mitel (now Zarlinc) as a prototype of a low-cost receiver for mass market applications based on the GP2000 chipset.<sup>7</sup> It comprises a GP2015 front-end chip, a DW9255 saw filter, a GP2021 12-channel correlator for L1 C/A code and carrier tracking, and an ARM60B 32-bit microprocessor. The chipset is similarly used in industrial receivers (e.g., CMC Allstar) but has more recently been superseded by the combined GP4020 correlator and microprocessor, which allows more tightly integrated receiver designs (Superstar II, SigTec MG5001).

Although the Orion receiver itself has never reached the commercial production stage, the open design information<sup>8</sup> and the temporary availability of a source code level software development kit have resulted in a variety of rebuilds by universities and research centers to support specialized scientific and technological applications. In the context of spaceborne navigation, the Orion receiver has been flown on Surrey's SNAP-1<sup>9</sup> nanosatellite and the U.S. Naval Academy's PCsat<sup>10</sup> nanosatellite. Dual front-end versions for attitude determination and pseudolite applications have been developed at Stanford University,<sup>11</sup> California, and Johnson Spaceflight Center,<sup>12</sup> Houston, Texas, and sounding rocket experiments have been performed by Cornell University,<sup>3</sup> Ithaca, New York, and the German Space Operations Center.<sup>6</sup>

The key receiver elements are combined on a single printed circuit board of  $95 \times 50$  mm size, which holds a 10-MHz temperature-compensated crystal oscillator, the front-end, correlator, and processor as well as RAM (512 kB) and ROM (256 kB) memory. At a regulated 5-V supply the receiver consumes a power of 2 W (or 2.4 W including typical switching regulator losses), which is a minor load for the onboard power systems of typical sounding rockets. The receiver provides two independent serial ports for communication with the telemetry and telecommand system or onboard data recorders. Finally, a discrete input pin is available to provide a lift-off signal to the GPS receiver. Using appropriate receiver software, this signal can be used to measure the accurate launch time and to compute auxiliary information that depends on the actual flight time (e.g., reference trajectory evaluation).

In the original receiver design the main board is complemented by an equally sized interface board providing support elements like a voltage regulator, RS232 line drivers, and a rechargeable backup battery for real-time clock operation and nonvolatile memory retention during off times. To comply with mission-specific space, power, and communication requirements, the auxiliary board has been replaced by a tailored version on most of the experimental sounding rocket flights conducted so far. As an example, Fig. 1 shows the Maxus-4 flight unit of the GPS Orion-HD receiver integrated by Kayser-Threde.

The GPS receiver hardware is complemented by a dedicated antenna system<sup>6</sup> made up of one or more passive antennas, optional radio frequency (RF) relays, and preamplifiers with a typical gain of 28 dB for each individual antenna string. While still on ground, an external antenna mounted at the launch pad and connected via the umbilical (or, alternatively, a reradiation device) is used to provide unobstructed GPS signals and ensure a proper initialization of the receiver.

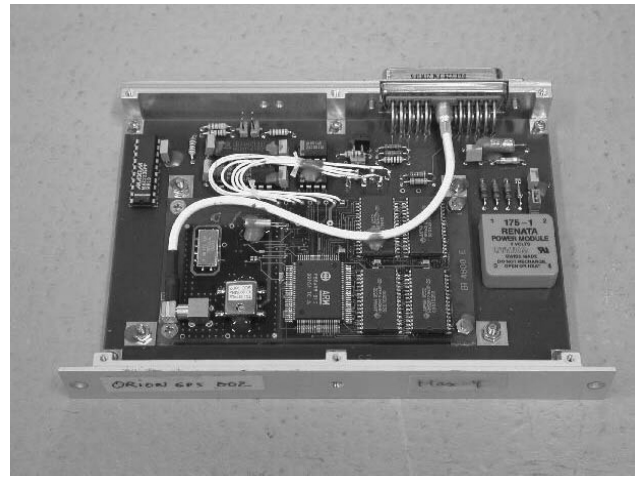


Fig. 1 Maxus-4 flight unit of the GPS Orion receiver with mission specific interface board (Kayser-Threde).



Fig. 2 Helical tip antenna with radome for GPS tracking of sounding rockets during the early flight phase (DLR Mobile Rocket Base).

During the early flight, the receiver is connected to a helical antenna in the tip of the ogive (Fig. 2), which ensures optimum visibility of the GPS constellation and makes the signal reception insensitive to spin about the longitudinal axis. The tip antenna is thus well suited to support the use of GPS as an IIP prediction system for range safety purposes.

After tip separation a dual-blade (or patch) antenna configuration has been proven to provide acceptable GPS tracking conditions even during the spin and reentry phase at considerably lower manufacturing and integration cost than traditional wrap-around antennas.

## III. GPS Receiver Software

A basic software for the GPS Orion receiver has earlier been made available by Mitel Semiconductor as part of the GPS Architect Development Kit.<sup>13</sup> In contrast to alternative GPS software packages for operation of GP2015/GP2021 cards inside a host PC (GPS Builder,<sup>14</sup> OpensourceGPS<sup>15</sup>), the GPS Architect software is specifically designed for use in a stand-alone GPS receiver employing the ARM60B microprocessor.

Despite its maturity, however, the GPS Architect code is essentially limited to terrestrial operations in a low-dynamics regime, and no effort has been made by the original developers to support its use in aerospace applications with intrinsically high velocities. Most notably, the prediction of line-of-sight Doppler shifts has therefore been modified by the authors to account for a nonnegligible receiver velocity, the navigation solution has been reformulated in terms of

Cartesian coordinates to avoid errors resulting from a neglected motion of the local horizontal frame in the spherical formulation, and the simple navigation filter assuming linear motion has been deactivated. Furthermore, a 1-ms timing error introduced by the bit-synchronization algorithm has been fixed.

To support a flexible operation of the receiver during prelaunch testing and in actual missions, numerous enhancements have been performed to the command and telemetry interface. Output messages can be freely configured in accord with the available downlink capacity. Both Nautical Marine Electronics Association (NMEA) type message formats and proprietary text message strings are supported. Other than the original Orion firmware, which collects measurements at equidistant but otherwise arbitrary time steps after power up, the revised software provides for an active alignment of measurements epochs and navigations solutions to integer GPS seconds with a representative accuracy of  $0.2 \mu\text{s}$  (selective availability off). Along with this, a hardware signal (pulse per second) of 1-ms duration is generated at the occurrence of each integer second that can be used for onboard clock synchronization purposes. Whereas raw measurements are internally collected at a 10-Hz sampling rate, the navigation solution and data output are performed at an update rate of either 1 or 2 Hz.

The high dynamics of the relative motion of user and GPS satellite as well as the rapidly varying GPS constellation visibility pose a major obstacle for the space-based use of a conventional GPS receiver. Dedicated modifications for high-dynamics applications have therefore been made, which include an open-loop aiding of the Doppler and visibility prediction<sup>5</sup> and the upgrade of the carrier-tracking loops.<sup>16</sup> In view of the low signal levels and the time-consuming correlation search process, special precautions have to be taken to achieve a rapid acquisition and an optimal channel allocation. This is readily accomplished by aiding the receiver with nominal trajectory information, if continuous GPS signal availability or operation of the receiver cannot be ensured. For sounding rockets or other ballistic missions the trajectory is represented by a piecewise, low-order polynomial approximation stored within the nonvolatile memory of the Orion-HD receiver. If code or carrier tracking should be lost during the flight, this information is used to compute the GPS satellites in view and the expected Doppler shift required to allocate and presteer the tracking channels.

After the initial signal acquisition the tracking performance of a GPS receiver under high dynamics depends crucially on the employed carrier-tracking loop. To follow the rapid frequency variations, the tracking loop should at least be of third order, in which case a constant acceleration can still be tracked without any steady-state error. Small loop filter bandwidths (implying a longer averaging of the tracked signal) are desirable to minimize the measurements noise, but also results in larger tracking errors in case of rapid frequency changes. A careful design and tuning of the tracking loop is therefore required to achieve the desired tracking accuracy both during the boost and free-flight phase.

The original Mitel Architect and Orion receiver software employs a second-order frequency-locked loop (FLL), which properly tracks the Doppler shift but cannot measure the instantaneous carrier phase. Furthermore, the particular implementation suffers from a signal strength dependent bandwidth, which makes it sensitive to dynamical stress in case of weak signals. The standard tracking loop has therefore been thoroughly revised and replaced by a third-order phase-locked loop (PLL) with FLL assist<sup>17</sup> that is fully described in Montenbruck.<sup>16</sup> To accommodate the increased dynamics encountered in sounding rocket applications, the loop bandwidth has been increased by a factor of four compared to terrestrial and low-Earth-orbit applications. This roughly doubles the carrier and Doppler noise but ensures stable tracking even in case of very high acceleration changes (start of boost, end of boost, reentry).

To ensure a reliable acquisition, the third-order PLL with FLL assist is only activated after proper frequency lock has been achieved with a pure second-order FLL using a cross-product discriminator with a wider pull-in range. Its estimates of frequency and frequency change are used to initialize the corresponding values of the third-order PLL prior to activation. In this way a robust acquisition of

carrier phase tracking is obtained. Both the second-order FLL and the third-order PLL do not exhibit acceleration-dependent steady-state errors and are sensitive only to high jerk. By combining both types of tracking loops, one benefits from a favorable acquisition performance and the availability of carrier phase measurements. These are used to compute smoothed pseudoranges based on a simple filter operated at a 10-Hz measurement update rate and a characteristic averaging time of 20 s. The smoothed pseudoranges are subsequently used to compute the single point position solution and clock offset correction, which thus exhibit a notably smaller noise level than in the unsmoothed case. Delta ranges derived from carrier phase measurements between consecutive epochs are furthermore used to obtain the line-of-sight range rates at the instance of the latest measurement and the corresponding velocity with a much smaller noise level than achieved with instantaneous Doppler measurements.

#### IV. IIP Prediction

Range safety at the launch site of a sounding rocket requires a continued monitoring of the instantaneous impact point. Following Koelle,<sup>18</sup> the IIP designates the expected landing point following an immediate termination of the boosted flight. It represents a contingency, in which the rocket motor is intentionally deactivated by the mission control center following a guidance problem or other failure error during the propelled flight phase. The real-time computation and display of the IIP allow the range safety officer to discern whether the rocket would eventually land outside the permissible range area and thus necessitate an abort of the boosted flight or even a destruction of the malfunctioning vehicle.

To comply with the restricted computational resources of common real-time systems, a simple, yet accurate, analytical IIP prediction method has been developed by the authors.<sup>19</sup> It is based on a plane-Earth parabolic trajectory model with first-order corrections for surface curvature, gravity variation and Earth rotation. Despite the implied simplifications, the resulting model is more complete and of higher accuracy than conventional IIP algorithms based on a flat-Earth approximation with Coriolis correction (e.g., see Regan et al.<sup>20</sup>). Overall, the agreement with the full modeling of conservative forces is high enough to introduce IIP prediction errors of less than 1.5% of the ground range for sounding rockets reaching altitudes of up to 700 km and flight times of about 15 min. On the other hand, the model is less complex than a perturbed Keplerian trajectory model or numerical integration and thus well suited for real-time computations.

For the description of the rocket trajectory, we employ a local horizontal coordinate system that is aligned with the instantaneous east, north, and up direction and originates in the foot point of the satellite at time  $t_0$ . Starting from the initial position  $s_0 = (0, 0, h_0)^T$  and velocity  $u_0 = (u_{0,E}, u_{0,N}, u_{0,up})^T$ , the sounding rocket performs a parabolic trajectory under the action of a constant vertical acceleration  $-g$  and impacts at

$$s = (u_{0,E}\tau, u_{0,N}\tau, 0)^T \quad (1)$$

after a flight time

$$\tau = (1/g) \left( u_{0,up} + \sqrt{u_{0,up}^2 + 2h_0g} \right) \quad (2)$$

A proper value of  $g$  is given by the effective surface acceleration<sup>21</sup>

$$g_{\text{eff}} = 9.7803[1 + 0.005279 \sin^2(\varphi)] \text{ m/s}^2 \quad (3)$$

which accounts for the cumulative effects of the Earth's central, centrifugal, and  $J_2$  attraction. For extended ground ranges  $d = (u_{0,E}^2 + u_{0,N}^2)^{1/2}\tau$ , the local horizontal plane is no longer a good approximation of the geoid, and the actual impact point is located at a negative height  $h = d^2/(2R_\oplus)$ . Along with an increase of the total flight time, the impact point is changed by a small amount:

$$\Delta s_{\text{IIP}} = \frac{(u_{0,E}^2 + u_{0,N}^2)\tau^2}{2R_\oplus} \begin{pmatrix} u_{0,E}/u_{\text{imp}} \\ u_{0,N}/u_{\text{imp}} \\ -1 \end{pmatrix} \quad (4)$$

where

$$u_{\text{imp}} = |\dot{h}(t_0 + \tau)| = -(u_{0,\text{up}} - g\tau) \quad (5)$$

is the magnitude of the vertical impact velocity.

In the following paragraphs linearized expressions are provided to account for various perturbations that are not considered in the parabolic approximation of the trajectory. A first correction is required to account for the Earth's rotation and the fact that the chosen reference frame is noninertial. This results in apparent forces known as centrifugal force (which is already considered in the effective gravitational acceleration) and the Coriolis force. Upon integrating the perturbing acceleration along the flight path, one obtains corrections to both the horizontal and vertical position components. Whereas the east and north components of the preceding expression translate directly into a corresponding correction of the predicted impact point coordinates, the vertical component implies an increment to the computed flight time and an associated extension of the ground track. Upon combining both terms, the total IIP correction for Coriolis forces is given by the expression<sup>19</sup>

$$\Delta s_{\text{IIP}} = \omega_{\oplus} \begin{pmatrix} +u_{0,N} \sin \varphi + (u_{0,E}^2 / u_{\text{imp}} - u_{0,\text{up}}) \cos \varphi \\ -u_{0,E} \sin \varphi + (u_{0,N} u_{0,E} / u_{\text{imp}}) \cos \varphi \\ 0 \end{pmatrix} \cdot \tau^2 + \frac{\omega_{\oplus} g}{3} \begin{pmatrix} \cos \varphi \\ 0 \\ 0 \end{pmatrix} \cdot \tau^3 \quad (6)$$

where  $\omega_{\oplus} = 0.729 \times 10^{-4}$  rad/s denotes the Earth's angular velocity. The along-track shift of the IIP caused by the change in flight time (i.e., terms proportional to  $u_{0,E}/u_{\text{imp}}$ ), which is commonly ignored in the discussion of the Coriolis correction, is mainly relevant for a rocket launched in an eastern or western direction, whereas it has no effect for northbound or southbound trajectories.

A further correction is required to account for the nonconstant gravitational acceleration. Here two independent effects must be considered for extended ground ranges and high-altitude missions. First, the gravity vector is no longer perpendicular to the horizontal plane of the reference coordinate system, as the horizontal separation of the rocket from the initial foot point increases. This deflection of the plumb line results in an ever-increasing deceleration and an associated shortening of the impact range by

$$\Delta s_{\text{IIP}} = -\frac{g}{6R_{\oplus}} \begin{pmatrix} u_{0,E} \\ u_{0,N} \\ 0 \end{pmatrix} \tau^3 \quad (7)$$

Second, the decrease of the gravitational acceleration  $g$  with altitude  $h$  results in an increased flight time, which again increases the resulting flight range. By linear expansion and integration along the flight trajectory, one finally obtains the following expression for the associated IIP shift:

$$\Delta s_{\text{IIP}}(t_0) = \frac{1}{3R_{\oplus}} \frac{(h_0 + u_{0,\text{up}}\tau)(5h_0 + u_{0,\text{up}}\tau)}{u_{\text{imp}}} \begin{pmatrix} u_{0,E} \\ u_{0,N} \\ 0 \end{pmatrix} \quad (8)$$

The two effects described by Eqs. (7) and (8) are partly counteracting, which explains the reasonable accuracy of IIP predictions assuming a constant gravitational acceleration along the vertical. However, the net effect depends on the actual flight profile, and it is therefore advisable to always include the respective corrections.

In view of the employed linearizations, the preceding equations are best valid for trajectories with ground ranges and altitudes that are small compared to the radius of the Earth. In practice, good results have been obtained for peak altitudes of 700 km and flight times up to 15 min (Maxus, VS-40).<sup>19</sup> Here, the predicted IIP differs from more rigorous models by less than 1.5% of the ground range.

The perturbed parabolic IIP prediction model is simple enough to allow a computation of the instantaneous impact point inside the

**Table 1** Flight parameters for simulated VS-30 and Maxus scenarios

Parameter	VS30 (Cuma)	Maxus
Launch site	$\lambda = -44.4$ deg $\varphi = -2.3$ deg	$\lambda = +21.1$ deg $\varphi = +67.9$ deg
Boost duration	30 s	64 s
Flight time (to parachute)	415 s	870 s
Apogee altitude	180 km	710 km
Horizontal range	130 km	80 km
Max. velocity	1680 m/s	3330 m/s
Max. acceleration (ECEP)	12.1 g	12.5 g
Max. jerk	29 g/s	15 g/s

**\$PDLM,IIP,120228.50,1,6834.2656,N  
,02044.8612,E,0614.35\*17**

**Fig. 3** Example of an NMEA-compatible IIP data message providing the UTC time (12:02:28.5), the latitude (+68°34.2556'), and longitude (+20°44.8612') of the predicted instantaneous impact point as well as the expected time to impact (614.35 s) for a simulated Maxus trajectory originating from the Kiruna launch site.

Orion-HD GPS receiver at the 2-Hz navigation update rate. As a rule of thumb, 2–3% of the available ARM60B processing power is required for the IIP computation as compared to 5–10% for a single navigation solution. After converting the results from the instantaneous horizontal local vertical frame to the global WGS 84 systems, the geodetic impact point coordinates are output along with other navigation and status data. For compatibility with the NMEA standard, a special message format illustrated in Fig. 3 has been defined.

## V. Simulator Testing

To assess the navigation and IIP prediction performance of the Orion-HD GPS receiver, hardware-in-the-loop simulations have been carried out using a Spirent STR4760 GPS signal simulator. Two scenarios with notably different flight parameters were considered to cover a representative set of mission profiles: a VS-30 rocket launched from the Brazilian Alcantara site and a Maxus rocket launched from Esrange, Kiruna (Table 1). The VS-30 scenario is based on the Cuma mission, which used a single-stage S30 motor to carry its payload to a nominal apogee altitude of 180 km within 210 s from liftoff. During the 30-s boost phase, the rocket reaches an altitude of 31 km and builds up a speed of 1680 km/s with a peak acceleration of 12 g. After a flight time of approximately 415 s, the parachute is opened, and the payload ultimately touches down in the Atlantic Ocean at a distance of about 130 km east of the launch site. The second scenario represents the standard flight path of the Maxus rocket, which provides the main platform for the European microgravity program (Fig. 4). The guided rocket achieves an apogee altitude of roughly 700 km with an 800-kg payload using a single-stage Castor-4B booster and allows for a total  $\mu g$  time of 12 min.

In accord with restrictions of the Spirent signal simulator, simulation trajectories approximating the nominal flight profile for both scenarios have been modeled by a continuous sequence of third-order position polynomials representing piecewise constant jerk (acceleration rate) over time intervals of 0.1 to 5 s. The resulting acceleration and jerk profiles are illustrated in Fig. 5.

Maximum jerks of 29 and 15 g/s occur at boost start in the VS30/Cuma and Maxus scenario, respectively, whereas more moderate values of up to 4 g/s are encountered near boost termination. During the boost phase, the acceleration increases from 6 g (VS30/Cuma) and 2 g (Maxus) to a maximum of roughly 12 g in both missions.

A comparison of measured positions and velocities for the Maxus scenario with the simulated reference trajectory is shown in Fig. 6. In the absence of selective availability and broadcast ephemeris errors, the position determined by the Orion-HD GPS receiver exhibits an rms scatter of 0.1, 0.3, and 0.5 m in east, north, and up directions. Sudden jumps in the position solution at irregular intervals



**Fig. 4** Maxus rocket has an overall length of 15.8 m and a total mass of 11.4 tons. It employs a Morton Thiokol Castor 4B motor, which develops a thrust of 430 kN over a 64-s burn time.

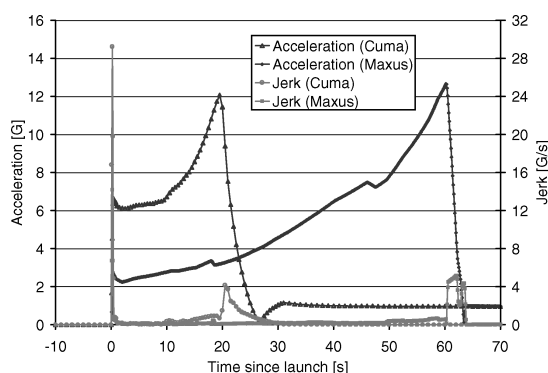


**Fig. 5** Total acceleration and jerk (in the Earth-fixed reference frame) for the simulated VS-30/Cuma and Maxus scenarios.

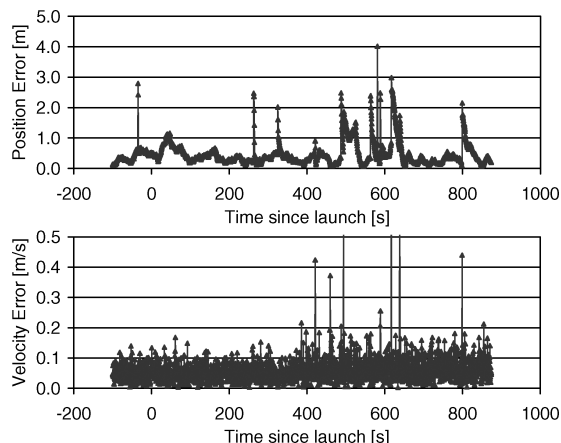


**Fig. 6** Position and velocity errors for simulated Maxus scenario in the absence of tropospheric and ionospheric path delays.

are caused by restarts of the carrier phase smoothing process on individual channels and reflect the inherent pseudorange accuracy of about 1 m.

The velocity noise amounts to roughly 2, 4, and 6 cm/s, respectively, in the east, north, and vertical axes, which includes contributions caused by carrier phase noise and simplifications in the onboard velocity solution. No indications of an acceleration or jerk dependence of the navigation solution are obvious from data collected during the boost phase of the simulated Maxus trajectory. In case of the VS30/Cuma scenario (which exhibits a two times higher initial jerk value), navigation solutions with a similar accuracy as in the Maxus scenario were collected throughout the flight.

Overall, the tracking performance is in good accord with results reported previously<sup>22</sup> for a less demanding low-Earth-orbit application with line-of-sight accelerations of up to 1 g. As a result of the increased tracking loop bandwidth, however, the carrier phase noise (0.8–1.5 mm) and range-rate noise (0.25–0.5 m/s) is somewhat larger than in the low-dynamics application.

Results of the IIP prediction performed within the Orion-HD GPS receiver are shown in Fig. 7 for the Maxus scenario. Compared to an off-line computation (using the true state vectors and a rigorous numerical trajectory integration accounting for all gravitational forces), the onboard IIP results differ by less than 2 km from the reference values, and even better results are obtained for the shorter VS30/Cuma flight range (Fig. 8).

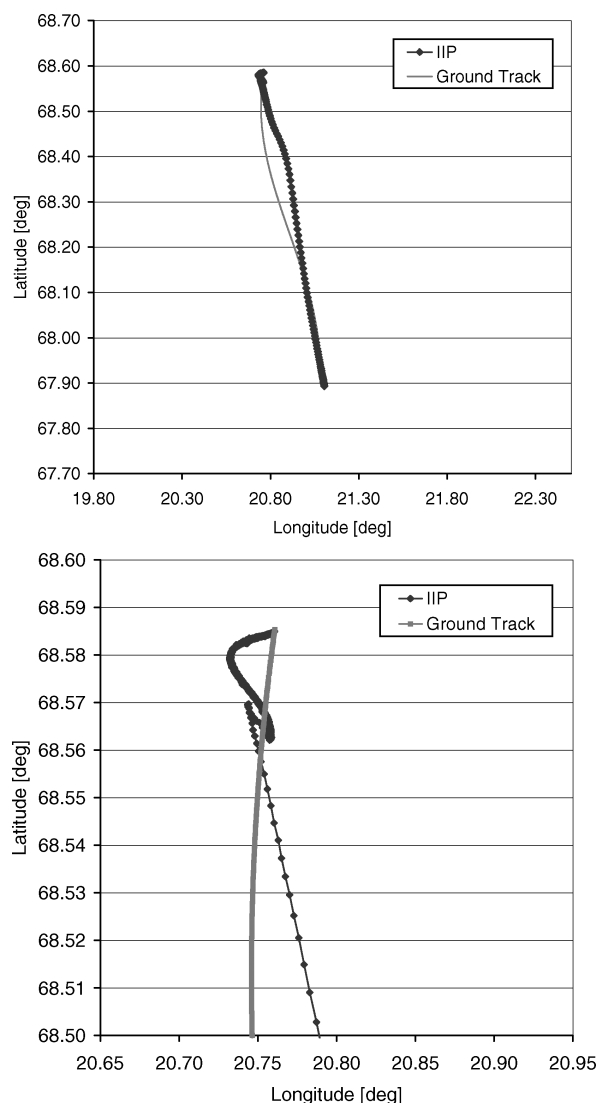


**Fig. 7** Onboard IIP results and ground track for simulated Maxus trajectory: top, complete flight path; bottom, close-up view of landing area). 0.01° in latitude corresponds to roughly 1 km.

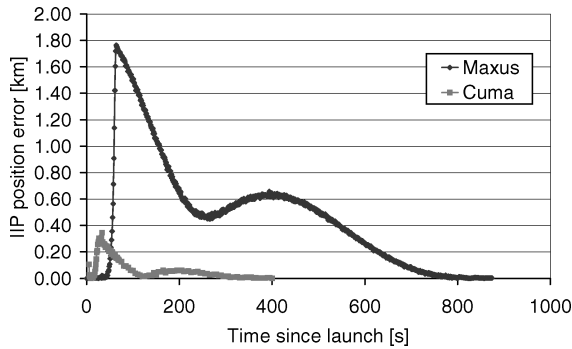


**Fig. 8 Error of onboard IIP prediction with respect to off-line IIP computation using true state vectors and numerical trajectory model (Maxus and VS30/Cuma scenarios).**

The onboard IIP prediction thus provides an adequate accuracy for range safety purposes and even slightly outperforms the operational, ground-based IIP prediction used at Esrange Kiruna.<sup>23</sup> It has to be emphasized, however, that the neglect of atmospheric drag and lift forces can ultimately introduce a much higher uncertainty than implied by the preceding figures.

## VI. Flight Results

The Maxus-5 sounding rocket was launched on 1 April 2003 from Esrange Kiruna. It carried a scientific payload of 795 kg and reached an altitude of 701 km with a total  $\mu g$  phase of 736 s. GPS tracking was provided by two independent receivers, an Ashtech G12 HDMA and an Orion-HD. Continuous GPS coverage from launch to landing was ensured by a three-stage antenna system. It comprised a tip antenna (employed during the boost phase), a single-patch antenna (can antenna) mounted on the parachute can (available after deployment of the nose cone), and, finally, a dual-patch antenna combination (used during the descent and reentry phase).

For redundancy, GPS data were transmitted to the ground via two independent S-band telemetry systems (payload and motor telemetry). The position and velocity measurements from both GPS receivers were used on ground to perform real-time predictions of the instantaneous impact point for range-safety purposes. In addition the onboard IIP prediction provided by the Orion receiver was transmitted as part of the telemetry data stream, but not yet used operationally.

In accord with the expected performance, the GPS measurements from both receivers agreed to 5 m and 0.5 m/s (three-dimensional rms) during the entire free-flight phase. Occasional outliers of up to 100 m and 10 m/s in the Orion-HD data can be attributed to an immature screening of bad pseudorange and range-rate measurements near the begin of track of new satellites. These (re-)acquisitions affect a single, low-elevation satellite during the boost phase but are otherwise most frequent during operation of the dual-patch antenna system, which suffers from pronounced gain drops at certain viewing angles. A more elaborate editing scheme is under consideration to reject bad measurements in future software versions.

No degradation of the tracking accuracy could be observed during the high jerk at boost end, where the acceleration dropped from 12 to 0 g in about 2.5 s. At the beginning of the reentry (with a peak jerk near 6.5 g and a significant spin of about 0.8 Hz), a brief outage (4 s) with invalid Orion-HD navigation data occurred. After reacquisition of all channels, the receiver yielded trustworthy navigation data through the reentry shock with a maximum deceleration of ca. 35 g. Because of a loss of tracking of the G12 receiver at spin-up, no GPS-based reference information is available during the final flight phase, and the performance assessment of the Orion-HD receiver is exclusively based on the consistency with onboard accelerometers.

Overall, the Orion-HD receiver provided reliable tracking for IIP prediction throughout all flight phases. Following Eq. (1), position errors translate directly into IIP errors, whereas the effect of velocity errors scales with the remaining time to impact. For the given

mission profile GPS measurement noise therefore contributes less than 0.5 km to the IIP prediction error, which is in fair accord with results reported for the Ballistic Missile Range Safety Technology (BMRST) system.<sup>24</sup> It should be emphasized, however, that the IIP error budget is dominated by uncertainties in the modeling of atmospheric drag,<sup>19</sup> compared to which the impact of GPS tracking errors can generally be neglected.

Results of the onboard IIP prediction performed by the Orion-HD receiver are shown in Fig. 9. After burnout of the Castor 4B engine, the predicted impact point matches the reentry point and the actual landing point within about 3 km. This underlines a good overall modeling of the free-flight trajectory in the simplified onboard IIP prediction algorithm.

For further comparison, Fig. 10 shows the results of other real-time IIP predictions used for operational range safety purposes

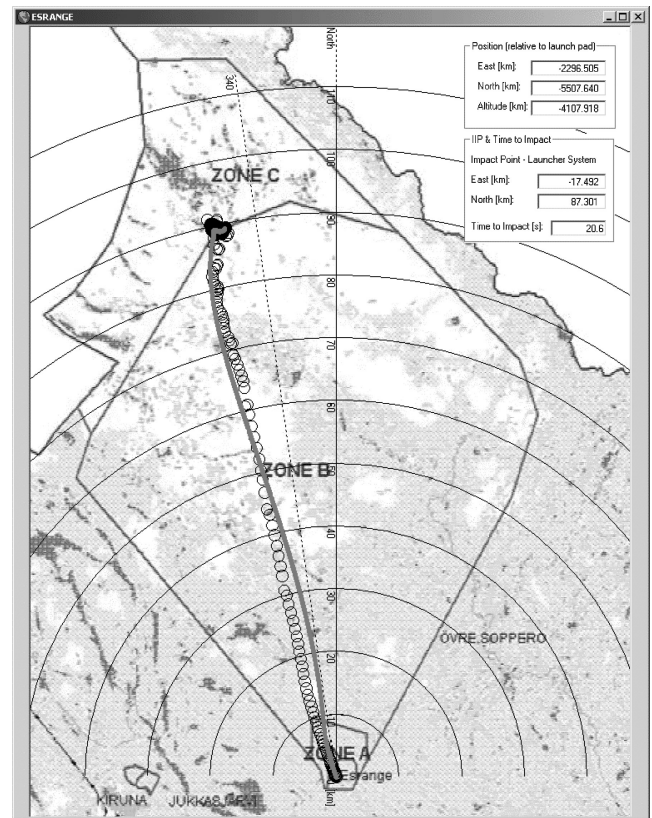


**Fig. 9 Plot of Maxus-5 ground track (—) and instantaneous impact point predictions (○) computed within the Orion-HD receiver.**

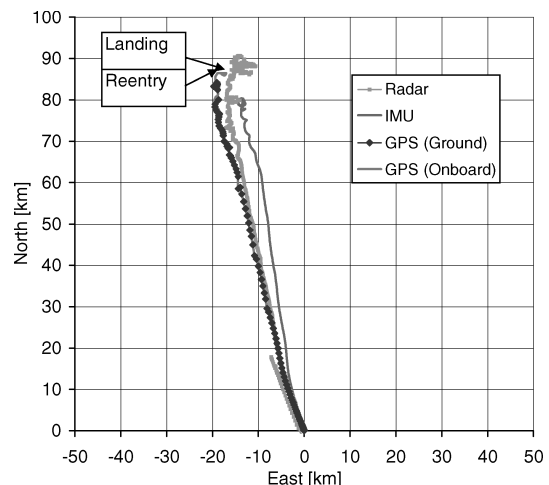


**Fig. 10 Comparison of IIP predictions for Maxus-5 using GPS, radar, and inertial platform (IMU) data.**

during the Maxus-5 mission. The IIP values computed inside the Orion-HD receiver are barely discernible from the GPS based predictions performed on ground. They notably outperform both the radar-based IIP predictions computed on ground and the onboard IIP predictions provided by the inertial measurement unit (IMU) of the Maxus guidance system.

## VII. Summary

The design and verification of the Orion-HD GPS receiver providing onboard IIP prediction for sounding rockets have been presented. Starting from a terrestrial low-cost receiver design, the GPS Orion-HD receiver has received numerous modifications for high-dynamics applications. Important enhancements include an aiding of the signal acquisition through coarse a priori trajectory data and the use of a third-order PLL with FLL assist that tolerates high accelerations. Furthermore, an analytical model for the prediction of the instantaneous impact point has been implemented in the receiver software. Starting from a simple parabolic trajectory model, various corrections are made to account for the curvature of the surface of the Earth as well as the integral effects of the Coriolis force and gravity field changes along the trajectory. Its accuracy is competitive with computationally more involved algorithms in existing range safety systems and can thus be used to make compatible IIP information available onboard the sounding rocket itself. Simulation results and actual flight data confirm the proper operation of the receiver concerning both the fundamental navigation accuracy and the onboard IIP prediction.

Compared to the BMRST system,<sup>24</sup> which employs an integrated GPS/IMU as well as a dedicated processor and RF transmitter in the space segment, the present solution is considerably less hardware intensive and makes a maximum reuse of existing onboard hardware. Despite its simplicity and low cost, the GPS-only solution has been shown to provide accurate IIP predictions in real-time and onboard the host vehicle. It is therefore considered as a valuable supplement for future onboard navigation systems of guided sounding rockets. Beyond the encouraging flight results obtained so far, further tests are under preparation to fully assess the robustness of Orion-HD receiver in critical situations and improve the overall maturity of the system.

## Acknowledgments

The test and qualification of the Orion-HD GPS receiver has extensively been supported by the Mobile Rocket Base of DLR/German Space Operations Center and by Kayser-Threde, Munich. The authors are grateful for the engineering work and flight opportunities provided by both parties. Access to GPS signal simulators during the development and test phase of the Orion-HD receiver has kindly been granted by Kayser-Threde and the Center for Space Research, Austin, Texas.

## References

- <sup>1</sup>Bull, B., "A Real Time Differential GPS Tracking System for NASA Sounding Rockets," *Proceedings of the ION-GPS-2000, 13th International Technical Meeting of the Institute of Navigation*, Inst. of Navigation, Fairfax, VA, 2000, pp. 2028–2037.
- <sup>2</sup>Montenbruck, O., Markgraf, M., Turner, P., Engler, W., and Schmitt, G., "GPS Tracking of Sounding Rockets—A European Perspective," *Proceedings of the NAVITECH'2001, 1st ESA Workshop on Satellite Navigation User Equipment Technologies*, ESA, Noordwijk, The Netherlands, 2002, pp. 378–385.
- <sup>3</sup>Powell, S. P., Klatt, E. M., and Kintner P. M., "Plasma Wave Interferometry Using GPS Positioning and Timing on a Formation of Three Sub-Orbital Payloads," *Proceedings of the ION-GPS-2002, 15th International Technical Meeting of the Institute of Navigation*, Inst. of Navigation, Fairfax, VA, 2002, pp. 145–154.
- <sup>4</sup>"Streamlining Space Launch Range Safety," National Research Council, Aeronautics and Space Engineering Board, National Academy Press, Washington, DC, 2000.
- <sup>5</sup>Montenbruck, O., Enderle, W., Schesny, M., Gabosch, V., Ricken, S., and Turner P., "Position-Velocity Aiding of a Mitel ORION Receiver for Sounding-Rocket Tracking," *Proceedings of the ION-GPS-2000, 13th International Technical Meeting of the Institute of Navigation*, Inst. of Navigation, Fairfax, VA, 2000, pp. 2003–2008.
- <sup>6</sup>Markgraf, M., Montenbruck, O., Hassenpflug, F., Turner, P., and Bull, B., "A Low Cost GPS System for Real-Time Tracking of Sounding Rockets," *Proceedings of the 15th European Symposium on European Rocket and Balloon Programmes and Related Research*, edited by B. Warmbein, ESA, Noordwijk, The Netherlands, 2001, pp. 495–502.
- <sup>7</sup>"GPS Orion 12 Channel GPS Receiver Design," Mitel Semiconductor, DS4808, Issue 1.3, Aug. 1997.
- <sup>8</sup>"GP2000 GPS Receiver Hardware Design," Mitel Semiconductor, AN4855, Issue 1.4, Feb. 1999.
- <sup>9</sup>Unwin, M. J., Palmer, P. L., Hashida, Y., and Underwood, C. I., "The SNAP-1 and Tsinghua-1 GPS Formation Flying Experiment," *Proceedings of the ION-GPS-2000, 13th International Technical Meeting of the Institute of Navigation*, Inst. of Navigation, Fairfax, VA, 2000, pp. 1608–1611.
- <sup>10</sup>Leung, S., Montenbruck, O., and Bruninga, R., "GPS Tracking of Microsatellites—PCsat Flight Experience," *Proceedings of the 5th International ESA Conference on Guidance, Navigation and Control Systems*, edited by R. Harris, ESA, Noordwijk, The Netherlands, 2002, pp. 423–430.
- <sup>11</sup>Stone, J. M., LeMaster, E. A., Powell, J. D., and Rock, S. M., "GPS Pseudolite Transceivers and Their Applications," *Proceedings of the ION-NM-1999, National Technical Meeting of the Institute of Navigation*, Inst. of Navigation, Fairfax, VA, 1999, pp. 415–424.
- <sup>12</sup>Wawrzyniak, G., Lightsey, E. G., and Key, K., "Ground Experimentation of a Pseudolite-Only Method for the Relative Positioning of Two Spacecraft," *Proceedings of the ION-GPS-2001 14th International Technical Meeting of the Institute of Navigation*, Inst. of Navigation, Fairfax, VA, 2001, pp. 1468–1478.
- <sup>13</sup>"GPS Architect Software Design Manual," Mitel Semiconductor, DM000066, Issue 2, April 1999.
- <sup>14</sup>"GPS Builder-2.1 12 Channel GPS Development System," GEC Plessey Semiconductors, DS4537, Issue 1.3, 1995.
- <sup>15</sup>Kelley, C., Cheng, J., and Barnes, J., "OpensourceGPS: Open Source Software for Learning About GPS," *Proceedings of the ION-GPS-2002, 15th International Technical Meeting of the Institute of Navigation*, Inst. of Navigation, Fairfax, VA, 2002, pp. 2524–2533.
- <sup>16</sup>Montenbruck, O., "A Discussion of FLL and PLL Tracking Loops for the Mitel Architect/Orion Receiver," *Deutsches Zentrum für Luft- und Raumfahrt, DLR-GSOC TN 02-01, Oberpfaffenhofen, Germany*, April 2002.
- <sup>17</sup>Ward, P., "Satellite Signal Acquisition and Tracking," *Understanding GPS Principles and Applications*, Artech House Publishers, Boston, 1996, Chap. 5.
- <sup>18</sup>Koelle, H. H., *Handbook of Astronautical Engineering*, McGraw-Hill, New York, 1961, pp. 28–105.
- <sup>19</sup>Montenbruck, O., Markgraf, M., Jung, W., Bull, B., and Engler, W., "GPS Based Prediction of the Instantaneous Impact Point for Sounding Rockets," *Aerospace Science and Technology*, Vol. 6, No. 4, 2002, pp. 283–294.
- <sup>20</sup>Regan, F. J., and Anandakrishnan, S. M., *Dynamics of Atmospheric Re-Entry*, AIAA Education Series, AIAA, Washington, DC, 1993.
- <sup>21</sup>Moritz, H., "Geodetic Reference System 1980," *Bulletin Géoésique*, Vol. 62, No. 3, 1988, pp. 348–358.
- <sup>22</sup>Montenbruck, O., and Holt, G., "Spaceborne GPS Receiver Performance Testing," *Deutsches Zentrum für Luft- und Raumfahrt, DLR-GSOC TN 02-04, Oberpfaffenhofen, Germany*, May 2002.
- <sup>23</sup>Anderson, L., "Comparison Between IIP computed with SAAB Algorithm and IIP from Reference Data," Swedish Space Corp., DOX-RBE-#14255, Ver. 1.0, 2002/10/31, Esrange, Kiruna, Sweden, Oct. 2002.
- <sup>24</sup>Slivinsky, S., Nesbit, C., Bartone, Ch. G., Phillips, R., and Rexrode, R., "Development and Demonstration of a Ballistic Missile Range Safety Technology System," *Navigation—Journal of the Institute of Navigation*, Vol. 49, No. 2, 2002, pp. 91–102.

C. McLaughlin  
Associate Editor